



High-throughput screening based identification of small molecule antagonists of integrin CD11b/CD18 ligand binding

Mohd Hafeez Faridi^{a,1}, Dony Maignel^{a,1}, Brock T. Brown^b, Eigo Suyama^b, Constantinos J. Barth^a, Michael Hedrick^b, Stefan Vasile^b, Eduard Sergienko^b, Stephan Schürer^{c,*}, Vineet Gupta^{a,d,*}

^a Peggy and Harold Katz Family Drug Discovery Center, Division of Nephrology and Hypertension, Department of Medicine, University of Miami, Miami, FL 33136, USA

^b Burnham Center for Chemical Genomics, Sanford-Burnham Institute for Medical Research, 10901 North Torrey Pines Rd., La Jolla, CA 92037, USA

^c Department of Pharmacology and Center for Computational Science, University of Miami, Miami, FL 33176, USA

^d Department of Biochemistry and Molecular Biology, University of Miami, Miami, FL 33136, USA

ARTICLE INFO

Article history:

Received 22 February 2010

Available online 25 February 2010

Keywords:

Integrin
CD11b/CD18
Inhibitor
Screening
HTS assay
Adhesion assay

ABSTRACT

Binding of leukocyte specific integrin CD11b/CD18 to its physiologic ligands is important for the development of normal immune response *in vivo*. Integrin CD11b/CD18 is also a key cellular effector of various inflammatory and autoimmune diseases. However, small molecules selectively inhibiting the function of integrin CD11b/CD18 are currently lacking. We used a newly described cell-based high-throughput screening assay to identify a number of highly potent antagonists of integrin CD11b/CD18 from chemical libraries containing >100,000 unique compounds. Computational analyses suggest that the identified compounds cluster into several different chemical classes. A number of the newly identified compounds blocked adhesion of wild-type mouse neutrophils to CD11b/CD18 ligand fibrinogen. Mapping the most active compounds against chemical fingerprints of known antagonists of related integrin CD11a/CD18 shows little structural similarity, suggesting that the newly identified compounds are novel and unique.

© 2010 Elsevier Inc. All rights reserved.

1. Introduction

Integrins are heterodimeric receptors composed of non-covalently linked α - and β -chains that mediate cell-adhesion, migration and signaling [1]. The β 2 family of integrins has a common β -chain (β 2, CD18) and one of four different α -chains (CD11a, CD11b, CD11c and CD11d), which together form four distinct receptors. The β 2 integrin CD11b/CD18 (also known as complement receptor type 3 (CR3), Mac-1 and α M β 2) is primarily expressed on neutrophils, macrophages and monocytes, is critical for the normal function of these cells and plays an important role in the development of inflammatory response [2–4]. Integrin CD11b/CD18 recognizes a wide variety of physiologic ligands, including fibrinogen (Fg), the complement fragment iC3b and CD54 (ICAM-1). Binding of integrin CD11b/CD18 to its ligands is dependent on divalent cations and is tightly regulated *in vivo*. Integrin CD11b/CD18 is expressed in a low-affinity, inactive conformation in circulating leukocytes, but is rapidly upregulated on cell surface and activated to high-affinity, ac-

tive conformation on a sub-second timescale [5]. A loss of functional β 2 integrins in humans leads to leukocyte adhesion deficiency type 1, where circulating neutrophils fail to adhere to or migrate across the endothelium and the patients are susceptible to recurrent, life-threatening bacterial infections [2–4]. Conversely, inappropriate excessive activation of leukocyte integrins is also harmful, which contributes to sustained inflammation, ischemia–reperfusion injury [1,2], tissue damage [6], stroke [7], neointimal thickening in response to vascular injury [8] and the development of various autoimmune diseases [9], making it an important therapeutic target [10].

Indeed, blocking antibodies that prevent cell-adhesion have been effective in animal models of a number of inflammatory diseases [11,12]. However, the humanized anti-integrin blocking antibodies failed to show much benefit in a number of clinical studies [13]. Additionally, adverse effects due to the nonselective blockade of various other leukocyte functions by mAbs further complicates their use as a therapeutic agent [14]. Similarly, ligand mimics, such as recombinant glycoprotein neutrophil inhibitory factor (NIF) while effective in animals, was clinically ineffective in a phase II trial and was abandoned [15]. Recombinant proteins, such as the ligand-binding A-domain (also known as I domain) of CD11b that act as competitive antagonists have shown promising results in animals, but have yet to be tested in human studies [16]. Competitive ligand-mimetic peptides derived either from CD11b/CD18 ligands or anti-CD11b/CD18 mAbs were reported to be ineffective

* Corresponding authors. Present addresses: Center for Computational Science, University of Miami, Miami, FL 33176, USA (S. Schürer); Division of Nephrology and Hypertension, Miller School of Medicine, University of Miami, Miami, FL 33136, USA. Fax: +1 305 243 3209 (V. Gupta).

E-mail addresses: sschurer@med.miami.edu (S. Schürer), vgupta2@med.miami.edu (V. Gupta).

¹ Equal first authors.

in blocking ligand binding *in vitro* [17]. Thus, integrin CD11b/CD18 selective small molecules may be more promising therapeutic agents, especially compounds that target allosteric regulatory sites, such as the hydrophobic pocket known as site-for-isoleucine (SI-LEN) in CD11b/CD18 [18] (termed lovastatin binding site (L-site) [19] or I domain allosteric site (IDAS) [20] in related integrin CD11a/CD18). In fact, several small molecule antagonists targeting IDAS in integrin CD11a/CD18 have been reported (reviewed in [21]). Although a number of integrin CD11a/CD18 antagonists cross-react with integrin CD11b/CD18 and block its function, there are very few reports of antagonists targeting integrin CD11b/CD18 [22], primarily due to the lack of good high-throughput screening (HTS) assays with integrin CD11b/CD18. We recently described a novel cell-adhesion based HTS assay using the 384-well plate format that is ideal for the discovery of small molecule integrin CD11b/CD18 antagonists [23]. In this communication, we describe the discovery of several novel small molecule antagonists of integrin CD11b/CD18 using a modification of this HTS assay. Many of the newly identified compounds show high potency (IC_{50} of $<1 \mu M$). The compounds show little structural similarity to known integrin CD11a/CD18 antagonists. Using chemical clustering analyses, we also identified potential lead compounds for development into potential therapeutics in the future.

2. Materials and methods

Details of the assay reagents and the HTS assay methods are presented in associated [Supplementary materials](#).

2.1. Activity scoring and hit identification

Cell-adhesion under positive and negative control conditions was used to define the activity scale; signal corresponding to the number of non-small molecule treated cells adherent in activating buffer condition (in the presence of Mn^{2+} ions as agonist, PC) was considered maximum (100% binding) and the signal corresponding to the number of non-small molecule treated cells adherent in basal buffer condition (in the presence of 1 mM each of Ca^{2+} and Mg^{2+} , NC) was considered minimum (0% binding). Percent inhibition (or activity) for compounds was calculated on this scale using the following formula (where A represents the measurement from compound treated wells):

$$\% \text{ Inhibitor} = \frac{(PC - A)}{(PC - NC)} \times 100$$

Compounds with $\geq 50\%$ inhibition ($\geq 50\%$ activity) of cell-adhesion in the primary screen were selected as primary positives. The primary positives were cherry picked and retested in the assay at the same concentration ($10 \mu M$). In the screen with $\sim 92,500$ compounds, the primary positives that resulted in $\geq 40\%$ inhibition ($\geq 40\%$ activity) in the confirmatory screen were considered active and were used to generate dose–response curves.

Dose–response data were fitted to the Hill equation and the IC_{50} values (concentration needed for 50% inhibition of cell-adhesion) were calculated with GraphPad Prism (San Diego, CA) with four parameter logistic curve fitting, as previously described [23]. EC_{50} values (concentration needed for half-maximal increase in cell-adhesion) were similarly determined. All data are reported as mean \pm SD. Z' -factor was calculated as previous described [24].

2.2. Data sets and data aggregation

The integrin CD11b/CD18 ligand binding antagonist screening data from primary (Pubchem Assay ID (AID) 1497), confirmatory and dose–response assays was aggregated into one dataset. To

evaluate cell toxicity we used two additional data sets available in Pubchem, one against Jurkat cells (AIDs 364, 463, 464) and the other against HT1018 cells (AID 620). Unique chemical structure representations for the compounds in the aggregated dataset were generated using an in-house Scitegic Pipeline Pilot [25] protocol to remove salt forms (or other addends), generate consistent protonation states (at pH 7.4) and charge representations, standardize stereochemical representations, and canonicalize tautomers. Dose–response data was converted into pIC_{50} values ($-\log_{10}[IC_{50}]$ in molar concentration unit) and the datasets were subsequently aggregated by averaging exact values of the same measure. Various physicochemical descriptors for compounds were calculated using the Accelrys predictors implemented in Pipeline Pilot.

2.3. Compound clustering

Chemical series corresponding to the most active compounds were generated using Leadscape [26]. Structures of all 63 structurally unique compounds with $pIC_{50} \geq 6$ ($IC_{50} \leq 1 \mu M$) were enriched by adding compounds that are greater than 60% similar using Leadscape keys (and the Tanimoto metric). To remove redundancies and to obtain unique structurally homogeneous classes, the resulting compounds were clustered (via hierarchical agglomerative clustering, average linkage, Leadscape keys) using a cluster height of 0.5. For each cluster the average activity of the antagonist and the cell proliferation results were also calculated. The z-scores for the antagonist HTS assay results is defined as the number of standard deviations that the cluster average is away from the global average of the data set.

2.4. Neutrophil adhesion assay

Neutrophils from 8- to 10-week old WT B6 mice were isolated from thioglycollate-stimulated peritonea according to literature protocols [27]. Cells were suspended in TBS containing 0.5% gelatin and transferred to ligand-coated wells. Cells were incubated with $5 \mu M$ antagonists, in the presence of agonists Mn^{2+} ions (0.1 mM) or PMA (15 nM), for 10 min at $37^\circ C$. Subsequently, the assay plates were gently inverted for 30 min at room-temperature to dislodge the non-adherent cells. Cells remaining adherent were quantitated using imaging microscopy, as previously described [23,28]. Assays were performed in triplicate wells.

3. Results and discussion

3.1. HTS screening of chemical libraries against integrin CD11b/CD18

We used a cell-based adhesion assay using erythroleukemic K562 cells stably transfected with the wild type integrin CD11b/CD18 (K562 CD11b/CD18) in our screening assays, as previously described [23]. Wild type integrin is expressed in an inactive state in this cell line [29], but can be activated by inside-out signals or by Mn^{2+} ions primarily through a change in integrin affinity rather than avidity [30], thus providing an excellent context for the discovery of small molecule inhibitors of integrins [29]. In the adhesion assay, K562 CD11b/CD18 show minimal adhesion to fibrinogen (Fg) immobilized on 384-well plates in assay buffer (Tris-buffered saline (TBS)) containing physiologic 1 mM Ca^{2+} and 1 mM Mg^{2+} ions (conditions that maintain integrin in a low-affinity conformation). However, K562 CD11b/CD18 cells show high binding to the immobilized ligand in the presence of agonist Mn^{2+} ions in the assay buffer (conditions that convert integrin into a high-affinity conformation). As shown in Fig. 1A, Mn^{2+} ions induce K562 CD11b/CD18 cell-adhesion to Fg in a dose dependent fashion, with an apparent EC_{50} value of $65 \mu M$ in this assay, in

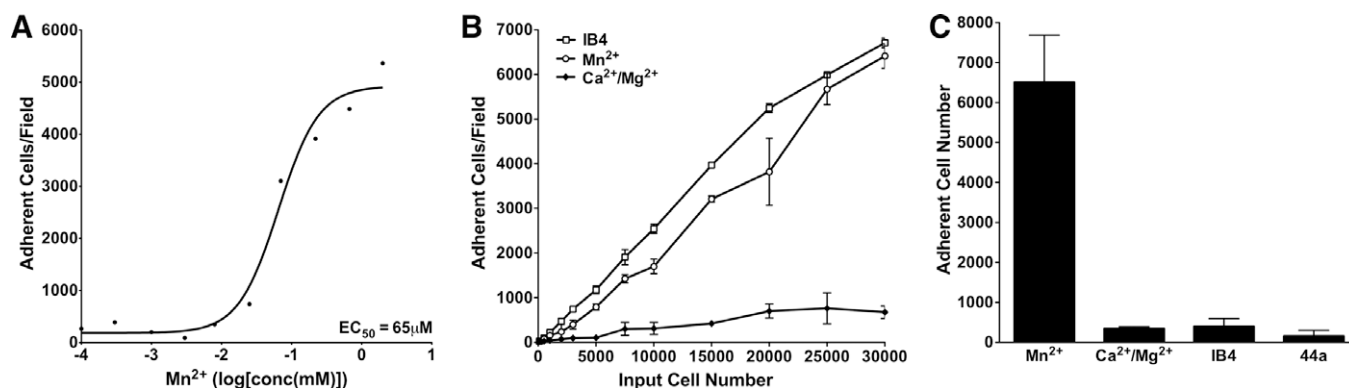


Fig. 1. Characteristics of the cell-adhesion based HTS assay. (A) A dose-response curve showing K562 CD11b/CD18 cell-adhesion to immobilized Fg in response to increasing concentration of activating Mn^{2+} ions. Mn^{2+} concentration is along the x-axis (log-scale) and the number of adherent cells (determined using automated microscopy [23]) is along the y-axis. Curve fitting was done using Graphpad Prism and the calculated EC_{50} value is shown. (B) A graph showing the number of adherent cells (y-axis) as a function of increasing number of input cells (x-axis) under three different the assay conditions- the immobilized antibody IB4 (which captures majority of input K562 CD11b/CD18 cells), 1 mM each of Ca^{2+} and Mg^{2+} ions (to determine background levels of cell-adhesion under non-activating conditions) and 1 mM Mn^{2+} ions (to determine number of cells adherent under activating conditions). Each point represents mean \pm SD of triplicate determinations. (C) A bar graph showing inhibition of agonist Mn^{2+} induced cell-adhesion by blocking mAbs. Cells were incubated in the presence of Mn^{2+} ions (1 mM), Ca^{2+} and Mg^{2+} ions (1 mM of each) or Mn^{2+} ions (1 mM) and blocking mAbs IB4 or 44a for 30 min at 37 $^{\circ}$ C in assay wells coated with ligand Fg. Each bar represents mean \pm SD of three to six determinations.

agreement with literature values with other integrins [31]. Additionally, as shown in Fig. 1B 80–90% of input cells (as measured by cell-adhesion to immobilized anti-CD18 mAb IB4 [32]) showed binding in the presence of agonist Mn^{2+} ions from very low (500 cells) to very high (30,000) number of input cells per well, providing high signal and good dynamic range in the assay. Binding remained minimal at all cell concentrations in the presence of Ca^{2+} and Mg^{2+} ions. Furthermore, incubation with known integrin CD11b/CD18 antagonists, mAbs IB4 and 44a, also blocked the agonist Mn^{2+} ion induced binding to immobilized Fg (Fig. 1C), establishing that cell-adhesion is integrin CD11b/CD18 dependent [23].

First, we performed a pilot screen using a commercially available library of >10,500 small molecules to identify novel antagonists of integrin CD11b/CD18 (inhibitors of integrin-dependent cell-adhesion) using this assay. One hundred and one compounds significantly decreased adhesion ($\geq 50\%$ inhibition) of K562 CD11b/CD18 cells to immobilized Fg in the presence of agonist Mn^{2+} ions in duplicate wells and were identified as primary positives from this screen (hit-rate of <1%). We cherry picked the top

37 primary positive compounds that produced the highest level of decrease in Mn^{2+} induced cell-adhesion for validation. We found that 11 of the selected compounds showed more than 50% inhibition of cell-adhesion in the confirmatory assays and were confirmed as antagonists (hit confirmation rate of $\sim 30\%$). Assays with five compounds were inconclusive and the rest of the compounds showed no effect. The selected compounds inhibited K562 CD11b/CD18 adhesion to Fg in a dose dependent fashion, with IC_{50} values in the low micromolar range [23].

Next, we used this assay to screen a chemical library of approximately 92,500 compounds (part of the NIH Roadmap Initiative small molecule library collection at BCCG as part of MLSCN). The average Z' -factor value for the entire screen was 0.65, and every assay plate had acceptable Z' -factor values (≥ 0.5). The primary screening data is graphically presented in Fig. 2. Results of this assay have been deposited into the Pubchem [33]. In the primary screen, 1658 compounds showed $\geq 50\%$ inhibition of K562 CD11b/CD18 cell-adhesion to immobilized Fg in the presence of agonist Mn^{2+} ions and we identified them as primary positives

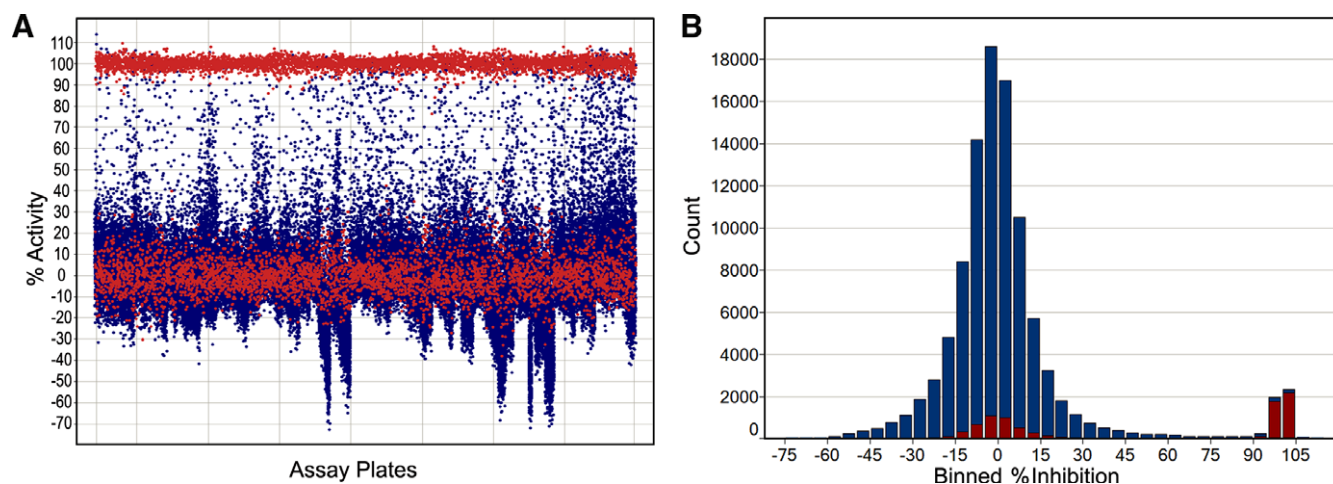


Fig. 2. High-throughput screening data for the integrin CD11b/CD18 antagonist assay using a chemical library of $\sim 92,500$ compounds. (A) A graph showing the raw experimental data. Each dot represents % activity measurement from an assay well. Blue colored dots represent measurements from compound treated wells and red colored dots represent measurements from positive and negative control wells. The graph was prepared using Spotfire software (Sommerville, MA). (B) A histogram showing a summary of percent inhibition (x-axis) by a number of compounds (y-axis). Percent inhibition was binned into 5% activity intervals. Percent inhibition from positive control and negative control wells is shown as red histogram. Percent activity from tested compounds is shown as blue histograms. (For interpretation of the references to color in this figure legend, the reader is referred to the web version of this article.)

from this screen (hit-rate of $\sim 1.8\%$). All 1658 compounds were cherry picked from the diluted compound plates used to generate the original primary screening data and retested in the assay. Of the 1658 compounds, 456 reproduced (showed $\geq 40\%$ activity) and were ordered from the NIH small molecule repository (hit confirmation rate of 27.5%). We identified these as secondary positives. We obtained 394 of the secondary positives from the repository and used them in a dose–response study. Compounds were tested in duplicate at 7–10 different concentrations (twofold dilution series) to generate the dose–response curves and the IC_{50} values for each compound. Additionally, the majority of the compounds were tested in three independent dose–response assays to determine the IC_{50} values with high confidence. Three hundred and eighty-three of the 394 secondary positives showed an average IC_{50} value of $<10 \mu M$ and were confirmed as antagonist hits (97% secondary hit confirmation rate). Sixty-three unique compounds showed sub-micromolar binding ($pIC_{50} \geq 6$, corresponding to $IC_{50} \leq 1 \mu M$), and are shown in Table S2. In comparison, lovastatin a known antagonist of the related integrin CD11a/CD18, is reported to have an IC_{50} of $25 \mu M$ in similar cell-based assays [20].

3.2. Compound clustering and identification of enriched structural motifs

In order to analyze the newly identified antagonists we aggregated the primary, confirmatory and dose–response data into a

single dataset. Furthermore, we added screening data from additional Pubchem assays, one against Jurkat cells and the other against HT1018 cells, to this dataset in order to evaluate possible cellular toxicity of the identified compounds, as previously described [34]. We generated unique chemical structure representations, as described in Section 2, and all resulting data was aggregated by unique structures.

Next, we used cheminformatics application Leadscape to generate activity-enriched clusters of structurally similar compounds [35]. Similarity clusters were built around seed compounds with $IC_{50} \leq 1 \mu M$ followed by hierarchical clustering to remove redundancy and scoring of the unique structurally homogeneous clusters as described in Section 2. Table S1 shows the resulting 45 unique compound series and a group of 17 singletons along with the activity (pIC_{50} value) and potential cytotoxicity for each group. Various physicochemical descriptors (such as surface area and volume, aqueous solubility, partition coefficient between *n*-octanol and water ($c \log P$), passive intestinal absorption) were also calculated for the identified antagonists using the predictors from Accelrys (not shown). Although cytotoxicity data are not available for all positive compounds, the presence of toxicity data for one or some compounds in a cluster can be a starting point to evaluate potential toxicity of a class of compounds. For example cluster 1 is among the most active, however at least one compound shows toxicity against Jurkat cells at sub-micromolar concentrations. The same is the case for cluster 2. Although cytotoxicity data is not available for cluster 3, the two trifluoro-methyl groups may make the com-

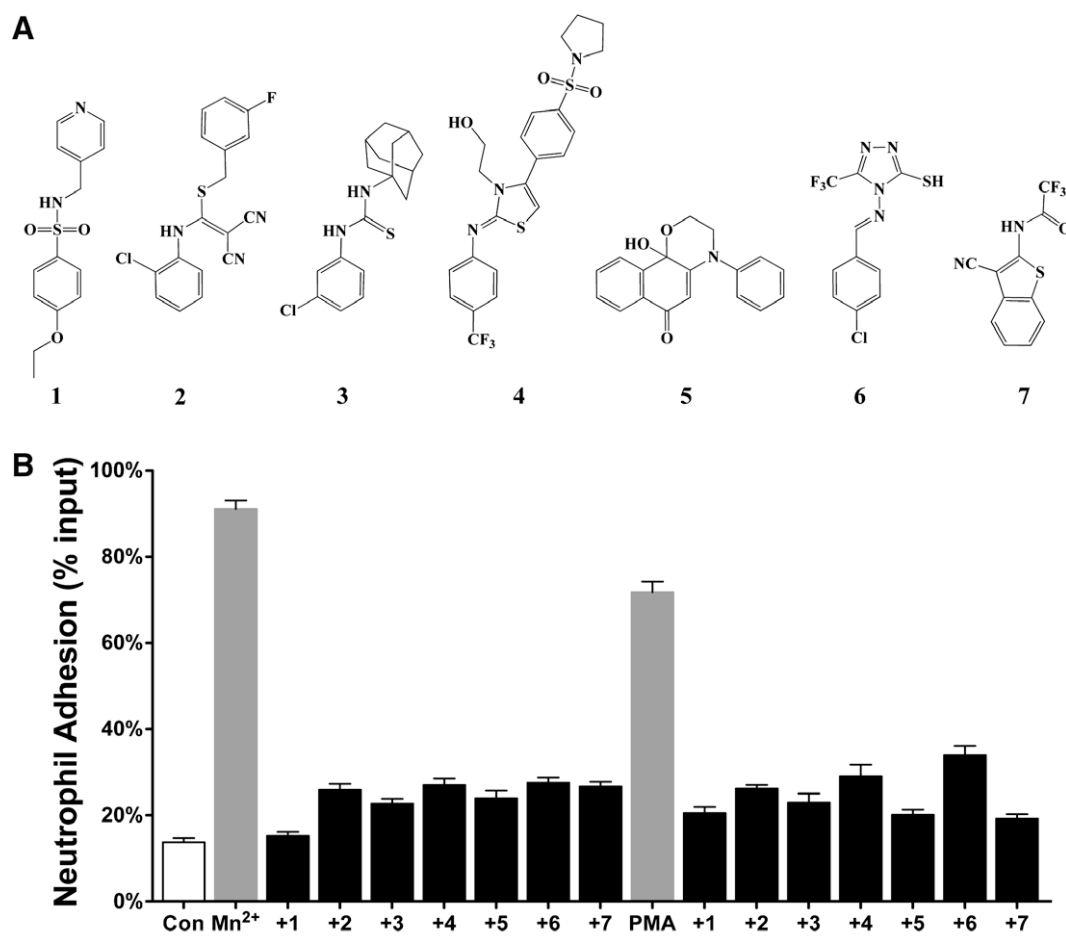


Fig. 3. Novel compounds inhibit CD11b/CD18 dependent adhesion of mouse neutrophils. (A) Chemical structures of identified hit compounds. (B) A histogram showing adhesion of mouse neutrophils to immobilized Fg in the control physiologic buffer containing 1 mM Ca²⁺ and Mg²⁺ (Con), with agonists (Mn²⁺ and PMA), and with agonists in the presence of one of the newly identified antagonists.

pounds less soluble (predicted aqueous solubility <0.1 to 1 μM) and thus not as attractive. Compounds of cluster 6 and 7 also have similar (calculated) properties. Likewise, the highly conjugated aromatic compounds of cluster 4 have low predicted aqueous solubility (<0.01 to 0.1 μM) and a $c \log P$ of close to 5. Compounds in cluster 38 appear interesting, but show some toxicity in the Jurkat cell assay. However, the sulfonamide compounds present in clusters 11 and 14 show high activity and an acceptable range of predicted physicochemical properties (aqueous solubility, $c \log P$, polar surface area, passive intestinal absorption). These compounds do not indicate obvious toxicity and their chemical structure suggests that their analogs could be readily synthesized for future structure–activity studies (SAR). For example, one compound (1, Fig. 3A, Pubchem SID 14720802) in cluster 14 is small, shows good antagonistic activity ($\text{IC}_{50} = 0.5 \pm 0.15 \mu\text{M}$), is a possible lead-series and a target for further optimization in the future.

To evaluate the novelty of the identified inhibitors, we compared structural similarity of all 383 identified antagonists with $\text{IC}_{50} \leq 10 \mu\text{M}$ to 11 of the structurally well-defined antagonists of related integrin CD11a/CD18 (see Supplementary methods). The results showing all similarity values of chemical fingerprints are in supporting Table S2. A histogram of the highest similarity value of each compound to any of the reference compounds is shown in Fig. S1. The results show that none of the 383 compounds have a similarity value >0.4, suggesting that our identified antagonists are structurally unique and novel. Structural comparison using extended connectivity functional group type fingerprints, instead of the atom type, ECFP4 fingerprints used for Fig. S1, yielded similar results. However, structural dissimilarity with known antagonists with a defined mechanism of action also prevents us from identifying potential mechanism of action for the identified antagonists.

3.3. Validation of hits using mouse neutrophils

The integrin CD11b/CD18 is primarily expressed on leukocytes. To examine the antagonistic activity of the identified hit compounds in a physiologically relevant cell type, we purchased a number of identified hits [23] (Fig. 3A) in a powder form and tested them for their effect on neutrophil cell-adhesion. All of the seven selected compounds had shown high antagonistic activity in the HTS assays [23,33]. WT B6 mouse neutrophils did not bind to immobilized CD11b/CD18 ligand fibrinogen (Fg) under physiologic conditions. However, integrin activation using divalent Mn^{2+} ions or PKC agonist phorbol 12-myristate 13-acetate (PMA) lead to dramatic increase in the neutrophil adhesion to Fg (Fig. 3B). We find that the novel antagonists potentially block agonists Mn^{2+} - and PMA-induced adhesion of mouse neutrophils to Fg (Fig. 3B).

In conclusion, we have identified a number of highly potent small molecule antagonists of integrin CD11b/CD18. Given that integrin CD11b/CD18 plays a key role in regulating leukocyte function, we believe that the newly identified antagonists will not only provide lead compounds for the development of potential therapeutics, but will also prove to be important new chemical biology tools for the study of the mechanism of integrin activation and function.

Acknowledgments

The authors thank Hiba Tannoury, Dr. Jun Y. Park and Dr. Jack Rosa for generous help and discussions with the cell-based assays; Dr. Thomas D. Y. Chung ("TC") and the staff of BCCG and Dr. Caroline Shamu and the staff of ICCB for their generous support in the implementation of the HTS assay and Prof. M. Amin Arnaout for helpful discussions. This work was supported in part by NIH Grants K01DK068253 and R03NS053659 and with resources of the Center for Computational Science at the University of Miami (#164). The MLSCN screening was performed by B.T.B., E.S., M.H., S.V. and E.S.

at Conrad Prebys Center for Chemical Genomics (CPCCG) and was supported through NIH Roadmap Grant U54HG003916. The chemical structure data tables in supporting Tables S1 and S2 were generated using ChemAxon JChem for Excel.

Appendix A. Supplementary data

Supplementary data associated with this article can be found, in the online version, at doi:10.1016/j.bbrc.2010.02.151.

References

- [1] R.O. Hynes, Integrins: bidirectional, allosteric signaling machines, *Cell* 110 (2002) 673–687.
- [2] M.A. Arnaout, Leukocyte adhesion molecules deficiency: its structural basis, pathophysiology and implications for modulating the inflammatory response, *Immunol. Rev.* 114 (1990) 145–180.
- [3] A.F. Horwitz, Integrins and health, *Sci. Am.* 276 (1997) 68–75.
- [4] A. McDowall, D. Inwald, B. Leitinger, A. Jones, R. Liesner, N. Klein, N. Hogg, A novel form of integrin dysfunction involving beta1, beta2, and beta3 integrins, *J. Clin. Invest.* 111 (2003) 51–60.
- [5] N. Hogg, B. Leitinger, Shape and shift changes related to the function of leukocyte integrins LFA-1 and Mac-1, *J. Leukoc. Biol.* 69 (2001) 893–898.
- [6] E.F. Plow, T.A. Haas, L. Zhang, J. Loftus, J.W. Smith, Ligand binding to integrins, *J. Biol. Chem.* 275 (2000) 21785–21788.
- [7] S.G. Soriano, A. Coxon, Y.F. Wang, M.P. Frosch, S.A. Lipton, P.R. Hickey, T.N. Mayadas, Mice deficient in Mac-1 (CD11b/CD18) are less susceptible to cerebral ischemia/reperfusion injury, *Stroke* 30 (1999) 134–139.
- [8] D.I. Simon, Z. Dhen, P. Seifert, E.R. Edelman, C.M. Ballantyne, C. Rogers, Decreased neointimal formation in Mac-1(–/–) mice reveals a role for inflammation in vascular repair after angioplasty, *J. Clin. Invest.* 105 (2000) 293–300.
- [9] T. Tang, A. Rosenkranz, K.J. Assmann, M.J. Goodman, J.C. Gutierrez-Ramos, M.C. Carroll, R.S. Cotran, T.N. Mayadas, A role for Mac-1 (CD11b/CD18) in immune complex-stimulated neutrophil function in vivo: Mac-1 deficiency abrogates sustained Fcgamma receptor-dependent neutrophil adhesion and complement-dependent proteinuria in acute glomerulonephritis, *J. Exp. Med.* 186 (1997) 1853–1863.
- [10] K. Yonekawa, J.M. Harlan, Targeting leukocyte integrins in human diseases, *J. Leukoc. Biol.* 77 (2005) 129–140.
- [11] H. Jaeschke, A. Farhood, A.P. Bautista, Z. Spolarics, J.J. Spitzer, C.W. Smith, Functional inactivation of neutrophils with a Mac-1 (CD11b/CD18) monoclonal antibody protects against ischemia–reperfusion injury in rat liver, *Hepatology* 17 (1993) 915–923.
- [12] C. Rogers, E.R. Edelman, D.I. Simon, A mAb to the beta2-leukocyte integrin Mac-1 (CD11b/CD18) reduces intimal thickening after angioplasty or stent implantation in rabbits, *Proc. Natl. Acad. Sci. USA* 95 (1998) 10134–10139.
- [13] A. Dove, CD18 trials disappoint again, *Nat. Biotechnol.* 18 (2000) 817–818.
- [14] C. Ramamoorthy, S.S. Sasaki, D.L. Su, S.R. Sharar, J.M. Harlan, R.K. Winn, CD18 adhesion blockade decreases bacterial clearance and neutrophil recruitment after intrapulmonary *E. coli*, but not after *S. aureus*, *J. Leukoc. Biol.* 61 (1997) 167–172.
- [15] M. Krams, K.R. Lees, W. Hacke, A.P. Grieve, J.M. Orgogozo, G.A. Ford, Acute stroke therapy by inhibition of neutrophils (ASTIN): an adaptive dose-response study of UK-279,276 in acute ischemic stroke, *Stroke* 34 (2003) 2543–2548.
- [16] K. Zerria, E. Jerbi, S. Hammami, A. Maaroufi, S. Boubaker, J.P. Xiong, M.A. Arnaout, D.M. Fathallah, Recombinant integrin CD11b A-domain blocks polymorphonuclear cells recruitment and protects against skeletal muscle inflammatory injury in the rat, *Immunology* 119 (2006) 431–440.
- [17] Y. Feng, D. Chung, L. Garrard, G. McEnroe, D. Lim, J. Scardina, K. McFadden, A. Guzzetta, A. Lam, J. Abraham, D. Liu, G. Endemann, Peptides derived from the complementarity-determining regions of anti-Mac-1 antibodies block intercellular adhesion molecule-1 interaction with Mac-1, *J. Biol. Chem.* 273 (1998) 5625–5630.
- [18] J.P. Xiong, R. Li, M. Essafi, T. Stehle, M.A. Arnaout, An isoleucine-based allosteric switch controls affinity and shape shifting in integrin CD11b A-domain, *J. Biol. Chem.* 275 (2000) 38762–38767.
- [19] J.R. Huth, E.T. Olejniczak, R. Mendoza, H. Liang, E.A. Harris, M.L. Lupher Jr., A.E. Wilson, S.W. Fesik, D.E. Staunton, NMR and mutagenesis evidence for an I domain allosteric site that regulates lymphocyte function-associated antigen 1 ligand binding, *Proc. Natl. Acad. Sci. USA* 97 (2000) 5231–5236.
- [20] J. Kallen, K. Welzenbach, P. Ramage, D. Geyl, R. Kriwacki, G. Legge, S. Cottens, G. Weitz-Schmidt, U. Hommel, Structural basis for LFA-1 inhibition upon lovastatin binding to the CD11a I-domain, *J. Mol. Biol.* 292 (1999) 1–9.
- [21] M. Shimaoka, T.A. Springer, Therapeutic antagonists and conformational regulation of integrin function, *Nat. Rev. Drug Discov.* 2 (2003) 703–716.
- [22] V.S. Bansal, S. Vaidya, E.P. Somers, M. Kanuga, D. Shevell, R. Weikel, P.A. Detmers, Small molecule antagonists of complement receptor type 3 block adhesion and adhesion-dependent oxidative burst in human polymorphonuclear leukocytes, *J. Pharmacol. Exp. Ther.* 304 (2003) 1016–1024.

- [23] J.Y. Park, M.A. Arnaout, V. Gupta, A simple, no-wash cell adhesion-based high-throughput assay for the discovery of small-molecule regulators of the integrin CD11b/CD18, *J. Biomol. Screen.* 12 (2007) 406–417.
- [24] J.H. Zhang, T.D. Chung, K.R. Oldenburg, A simple statistical parameter for use in evaluation and validation of high throughput screening assays, *J. Biomol. Screen.* 4 (1999) 67–73.
- [25] Pipeline Pilot 7.5, Accelrys, San Diego, 2009.
- [26] Leadscope Enterprise, Leadscope Inc., Columbus, 2007.
- [27] L.Y. Chen, J.J. Shieh, B. Lin, C.J. Pan, J.L. Gao, P.M. Murphy, T.F. Roe, S. Moses, J.M. Ward, E.J. Lee, H. Westphal, B.C. Mansfield, J.Y. Chou, Impaired glucose homeostasis, neutrophil trafficking and function in mice lacking the glucose-6-phosphate transporter, *Hum. Mol. Genet.* 12 (2003) 2547–2558.
- [28] W. Bergmeier, T. Goerge, H.W. Wang, J.R. Crittenden, A.C. Baldwin, S.M. Cifuni, D.E. Housman, A.M. Graybiel, D.D. Wagner, Mice lacking the signaling molecule CalDAG-GEFI represent a model for leukocyte adhesion deficiency type III, *J. Clin. Invest.* 117 (2007) 1699–1707.
- [29] S. Ortlepp, P.E. Stephens, N. Hogg, C.G. Figdor, M.K. Robinson, Antibodies that activate beta 2 integrins can generate different ligand binding states, *Eur. J. Immunol.* 25 (1995) 637–643.
- [30] C.R. Beals, A.C. Edwards, R.J. Gottschalk, T.W. Kuijpers, D.E. Staunton, CD18 activation epitopes induced by leukocyte activation, *J. Immunol.* 167 (2001) 6113–6122.
- [31] A. Masumoto, M.E. Hemler, Mutation of putative divalent cation sites in the alpha 4 subunit of the integrin VLA-4: distinct effects on adhesion to CS1/fibronectin, VCAM-1, and invasin, *J. Cell Biol.* 123 (1993) 245–253.
- [32] S.D. Wright, P.E. Rao, W.C. Van Voorhis, L.S. Craigmyle, K. Iida, M.A. Talle, E.F. Westberg, G. Goldstein, S.C. Silverstein, Identification of the C3bi receptor of human monocytes and macrophages by using monoclonal antibodies, *Proc. Natl. Acad. Sci. USA* 80 (1983) 5699–5703.
- [33] V. Gupta, HTS identification of compounds inhibiting the binding of CD11b/CD18 to fibrinogen via a luminescence assay. Pubchem Assay ID 1497, 2009.
- [34] R. Guha, S.C. Schurer, Utilizing high throughput screening data for predictive toxicology models: protocols and application to MLSCN assays, *J. Comput. Aided Mol. Des.* 22 (2008) 367–384.
- [35] P.E. Blower Jr., K.P. Cross, M.A. Fligner, G.J. Myatt, J.S. Verducci, C. Yang, Systematic analysis of large screening sets in drug discovery, *Curr. Drug Discov. Technol.* 1 (2004) 37–47.